# Thermosensitive Poly(*N*-isopropylacrylamide) Hydrogels Bonded on Cellulose Supports

**Jiangbing Xie, You-Lo Hsieh**

*Fiber and Polymer Science, University of California, Davis, California 95616*

Received 2 August 2002; accepted 21 October 2002

**ABSTRACT:** A two-step initiation and polymerization process was developed for the preparation of two series of hydrogel–cellulose composites with distinctively different morphologies and swelling behaviors. Hydroentangled cotton cellulose fibers were optimally initiated in 20 m*M* aqueous ammonium cerium(IV) nitrate for 15 min and then polymerized in aqueous solutions of *N*-isopropylacrylamide (NIPAAm) monomer and *N*,*N*′-methylene bisacrylamide (BisA) crosslinker. The extents of hydrogels on the cellulose solids could be controlled by variations in the concentrations of the monomer and crosslinker as well as the NIPAAm/BisA solution-to-solid ratios. The two series of hydrogel–cellulose composites formed were hydrogel-covered/filled cellulose (I) and cellulose-reinforced hydrogel (II) composites. Series I composites were synthesized with NIPAAm/BisA solutions below the liquid saturation level of the cellulose; this led to pore structures (size and porosity) that depended on both the extent and swelling of the grafted hydrogels. Series II composites were polymerized in the presence of excessive NIPAAm/BisA solutions to produce cellulose solids completely encapsulated in the hydrogels. All the cellulose-supported hydrogels exhibited lower extents of phase transition over a wider temperature range (28–40°C) than the free poly(*N*-isopropylacrylamide) hydrogels (32°C). These findings demonstrate that hydrogels can be used to control the pore structure of cellulose and can be supported with cellulose fibers. © 2003 Wiley Periodicals, Inc. J Appl Polym Sci 89: 999–1006, 2003

**Key words:** hydrogels; stimuli-sensitive polymers; composites

## INTRODUCTION

Hydrogels are three-dimensional networks of hydrophilic polymers that swell in the presence of water and shrink in the absence of water. Some hydrogels exhibit swelling behaviors in response to changes in the environment, such as the pH, temperature, ionic strength, electrical field, solvent, stress, and light. These stimuli-sensitive hydrogels have found important applications for drug delivery, switch control, mass separation, molecular recovery, and so forth. Much of the research on the formation, structures, properties, and applications of hydrogels has extensively been reviewed.[1–3]

The unique super-water-absorbing characteristic of hydrogels is also the reason for their poor mechanical and handling properties. To broaden their potential applications, we must overcome these limitations by improving their mechanical performance. One of the logical approaches is to reinforce hydrogels with solids, by either chemical bonding or physical entanglement. Chemical bonding has obvious advantages over physical means because of the strength and stability of covalent bonds. Polymer solids have been activated by ozone[4–8] and γ-irradiation[9,10] for the grafting of hydrogels. Ozone has been used to initiate the graft polymerization of hydroxyethyl methacrylate (HEMA),[4] acrylic acid,[5] and diethylene glycol methacrylate (DEGMA) hydrogels[6] on cellulose fibers and to form HEMA and DEGMA hydrogels on polypropylene membranes and fibers.[7] γ-irradiation has also been reported to initiate the polymerization of *N*-isopropylacrylamide (NIPAAm) hydrogels on cotton fabrics[9] and rubber.[10]

For cellulose, ceric ion is among the most effective chemical initiation techniques for the graft polymerization of vinyl monomers. Cerium(IV) is thought to oxidize cellulose to produce free radicals, which then initiate the polymerization of monomers present in the surrounding area. Evidence of complex formation between cerium(IV) and cellulose[11,12] has been reported. Disproportionation of the complex to generate free radicals has been proposed to be the rate-determining step for initiation.[13–15] The rate of polymerization was found to be inversely proportional to ceric ion concentrations; this suggests the termination of propagation by ceric ions.[16,17] With respect to the sites of free radicals on the cellulose, both the glycol groups at the C2–C3 position[14,15] and the hemiacetal unit[18,19] have been suggested. Reports on the grafting of three-dimensional networks with cerium(IV) have been limited to those on softwood pulp[20] and cellophane.[21]

*Correspondence to:* Y.-L. Hsieh (ylhsieh@ucdavis.edu).

Journal of Applied Polymer Science, Vol. 89, 999–1006 (2003)

The aim of this work is to demonstrate that a three-dimensional polymer network can be grafted onto cotton cellulose. Among all cellulose sources, cotton cellulose is the most challenging one for initiating reactions because it contains cellulose with the highest molecular weight, crystallinity, and orientation. NIPAAm, a thermosensitive vinyl monomer, is to be grafted onto cotton fibers through ceric-ion-initiated polymerization in the presence of a crosslinker. The effects of the initiation and polymerization on the formation and extent of the hydrogel network as well as the properties of the hydrogel–cellulose composites are investigated.

## EXPERIMENTAL

### Materials

*N,N′*-Methylene bisacrylamide (BisA) and ammonium cerium(IV) nitrate (CAN; Aldrich, St. Louis, MO) were used as received. NIPAAm (Acros, Pittsburgh, PA) was recrystallized from hexane/benzene (1:1 v/v). The cellulose solid used was hydroentangled cotton nonwoven (Cotton Inc., Cary, NC). The cotton cellulose was precleaned in boiling 1*M* NaOH for 1 h under $N_2$ and rinsed with water. It was further treated in 6*M* NaOH at 40°C for 1 h, then treated in 70% $ZnCl_2$ at room temperature for another 1 h, and finally rinsed with water. Purified water was used in all procedures.

### Hydrogel formation

All procedures, from the solution preparation to the graft polymerization, were performed at room temperature. Both the initiator (CAN) and monomer/crosslinker (NIPAAm/BisA) were dissolved in 0.1*M* aqueous $HNO_3$ and bubbled with $N_2$. Unless otherwise mentioned, cellulose (200 mg) was preweighted and initiated in 10 mL of 20 m*M* CAN for 15 min, blotted with tissues for the removal of extra CAN, and then immersed in 5 mL of an NIPAAm/BisA solution for 30 min. The reactant-impregnated cellulose was either spread on a dry glass dish (series I) or immersed in a 5-mL reactant solution in a 50-mL Pyrex beaker (series II). Substrates from both methods were polymerized under $N_2$ for 48 h. After the reaction, each substrate was rinsed with water for the removal of surface residues. The removal of the entrapped residues in the hydrogels was facilitated by three deswelling and swelling cycles, each in fresh water. Each cycle involved immersions in water at 45°C for 2 h and then in room-temperature water for 2 h, that is, above and below the lower critical solution temperature (LCST) of poly(*N*-isopropylacrylamide) (PNIPAAm). The cleaned samples were dried under vacuum at 80°C. The percentage of the hydrogel graft (*G*) on the cellulose support was calculated as follows:

$$G = (W_g - W_i)/W_i \times 100$$

where $W_i$ and $W_g$ are the sample weights before and after graft polymerization, respectively.

### Characterization

All swelling measurements were conducted in water at 25°C unless otherwise mentioned. The total swelling ratio ($q$) of the hydrogel–cellulose composite was calculated by the mass ratio of the fully hydrated weight ($W_h$) to the dry weight ($W_i$) of the sample:

$$q = W_h/W_i$$

The total pore volumes of the hydrogel–cellulose composites in fully hydrated and dry states were determined by liquid immersion. For the hydrated composites, the capillary water was removed by centrifugation at 3000 rpm for 5 min. Either the centrifuged or dried composite was immersed in hexadecane for 3 min to be fully saturated and weighed. The pore volume ($V_p$) was calculated as follows:

$$V_p = (W_a - W_b)/\rho_{\text{hexadecane}}$$

where $W_b$ and $W_a$ are the masses of the sample before and after immersion in hexadecane, respectively; $\rho_{\text{hexadecane}}$ is the density of hexadecane.

The thermal behaviors of the fully hydrated composites were measured by differential scanning calorimetry (DSC-50, Shimadzu; Columbia, MD) at a 2°C/min heating rate under $N_2$. Fiber and pore structures were examined with scanning electron microscopy (SEM; model DS 130, International Scientific Instrument). The samples were sputtered with gold, and the images were collected at 10 kV.

## RESULTS AND DISCUSSION

### Hydrogel formation

The initiation process of cellulose and the effects of the initiation on the graft polymerization of the monomer/crosslinker (NIPAAm/BisA) to form hydrogels were investigated first. Initiation of the cellulose solids was conducted either by a pretreatment process or simultaneously as part of the polymerization. As a pretreatment, the cleaned and swollen cellulose solids were immersed in the CAN initiator solution for a period of time before the monomer/crosslinker mixture was added. With simultaneous initiation and polymerization, the cellulose substrate was placed in the solution containing CAN, NIPAAm, and BisA as a batch reaction. The simultaneous introduction of the initiator with other reactants to cellulose did not yield observable amounts of hydrogels after 72 h. This re-

sult is in contrast to the batch reactions of the $Ce^{4+}$-initiated linear polymerization of acrylic monomers on cellulose, which usually showed high levels of grafting.[22,23] In our case in which the crosslinker BisA was present, some hydrogels were produced, but they appeared to be not substantially attached onto the solids. The pretreatment initiation led to the formation of PNIPAAm hydrogels on the cellulose substrates. Therefore, the two-step initiation and polymerization approach was employed for the remainder of this study.

In the two-step initiation and polymerization process, it was observed that, if an excessive CAN initiator solution was present in the reaction system, hydrogel formation on the solid was hindered. Noticeable amounts of hydrogels were formed on the cellulose only if the excessive CAN was removed by the blotting or rinsing of the initiator-saturated cellulose before the monomer/crosslinker solution was introduced. The ability of cerium(IV) to coordinate with vinyl monomers to form complexes and to initiate homopolymerization has been postulated.[24,25] Either complexation or homopolymerization consumes initiators and competes with graft polymerization. For efficient graft polymerization, therefore, the opportunity for the initiator to encounter monomers should be minimized. As observed here, separating the initiation and polymerization reactions as a two-step process and removing the excess CAN after initiation are both necessary. The relative contributions of homopolymerization and graft polymerization to cellulose are being studied in this laboratory, and the results will be described in a forthcoming publication.

Our attention was turned to find ways to control the extent of hydrogels on cellulose solids. First, the relative amount of the reactant solution to the substrate was varied. The CAN-initiated (20 m*M* CAN for 15 min) cellulose substrate was blotted with tissue and immersed in NIPAAm/BisA for 30 min. The NIPAAm/BisA-saturated cellulose was polymerized, either on a glass surface (method I) or in the presence of an additional NIPAAm/BisA solution (method II), for 48 h under $N_2$. With method I, the amount of grafted hydrogel was generally less than the mass of the substrate. About 1-mm-thick swollen hydrogel was observed mainly beneath the cellulose substrate on the glass side. The time taken to polymerize was sufficiently long to allow the aqueous reactant solution to settle underneath the substrate on the hydrophilic glass side. With method II, in which the polymerization proceeded with the solid surrounded by excess NIPAAm/BisA solution, the cellulose substrates were completely imbedded within the hydrogels formed. Much more hydrogel (>1 cm thick in the swollen state) could be grafted onto the solids, up to several times the mass of the cellulose. For both composite series, the hydrogels were attached to the substrates.

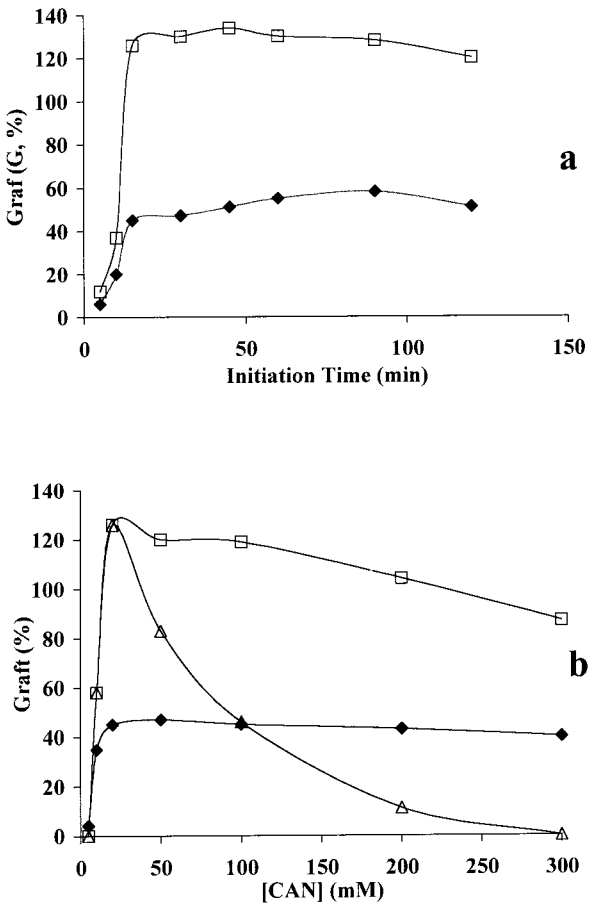


**Figure 1** Effects of the initiation conditions on PNIPAAm hydrogel formation on cellulose ([NIPAAm] = 2*M*; [BisA] = 0.04*M*) with (a) the initiation time ([CAN] = 20 m*M*) and (b) the initiator concentration (15 min): (♦) method I, (□) method II, and (△) method II without blotting.

For both methods, the initiation conditions affected the extent of the PNIPAAm hydrogel formed. The amounts of the hydrogels increased with the initiation time in the CAN solutions up to 15 min [Fig. 1(a)]. Prolonging the initiation time beyond 15 min resulted in no further production of hydrogels. At CAN concentrations below 5 m*M*, very little hydrogel was observed [Fig. 1(b)]. The amounts of the hydrogels increased most significantly when the CAN concentrations increased from 5 to 20 m*M*. Above 20 m*M*, a slightly decreasing trend for the hydrogels produced was observed. If the excess initiator solution was not removed, the grafts dropped dramatically with increasing initiator concentrations, going to zero at 300 m*M*. This is consistent with the earlier observation that excessive CAN solution inhibits gel formation on cellulose. A 15-min exposure to the 20 m*M* CAN solution was optimal for initiating the graft copolymerization of NIPAAm on cotton cellulose.

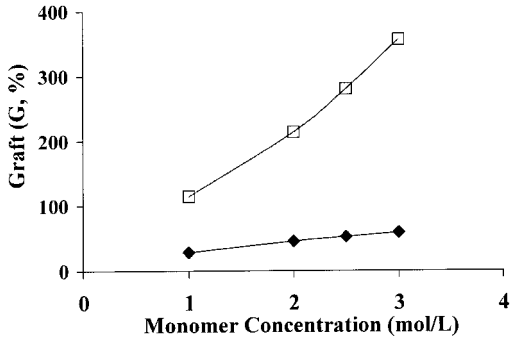


**Figure 2** Effect of the monomer concentration on *G* ([BisA] = 1.2% of [NIPAAm]): (♦) method I and (□) method II.

Under this optimized initiation condition, the quantities of hydrogels grafted onto cellulose increased with increasing monomer concentrations (Fig. 2). The concentration effects were much more pronounced with method II, in which excessive NIPAAm/BisA solution was present. The different monomer concentration effects of these two methods may be ascribed to the distinctly different morphologies of these two series of materials (to be discussed later).

The crosslinker BisA concentrations also affected the extents of grafting differently for the two methods. The extents of hydrogels generated by method I were essentially independent of the crosslinker BisA concentrations [Fig. 3(a)]. With method II, the amount of hydrogel peaked at 12 m*M*, or 1.2% of [NIPAAm], and then decreased with increasing BisA concentration. Although the grafting levels showed different trends with increasing BisA concentrations for these two methods, the *q* values of the hydrogel–cellulose composites decreased with increasing BisA concentrations in both series [Fig. 3(b)]. The reduced swelling was consistent with the expected increases in the crosslinking densities in the three-dimensional network structure.

An examination by SEM revealed two very distinct morphologies for these two series of hydrogel–cellulose composites (Fig. 4). Cotton cellulose fibers were randomly oriented by the hydroentanglement process and appeared to be mostly extended and straight [Fig. 4(a)]. Graft polymerization caused fibers to relax progressively with increasing extents of hydrogels. Series I composites showed various morphologies, from hydrogel-covered fibers to hydrogel-filled fibrous substrates [Fig. 4(b)]. At $G = 18\%$, the fibers were covered with very thin layers of hydrogels. At such a low grafting level, the twisted ribbon form of cotton fibers and their typical surface features, that is, the striations along the longitudinal direction, were still observable. As *G* reached 30%, the fibers were covered with thicker layers of hydrogels and became more cylindrical. The wrinkles or creases on the hydrogel-coated surfaces (shown by an arrow) appeared to be due to

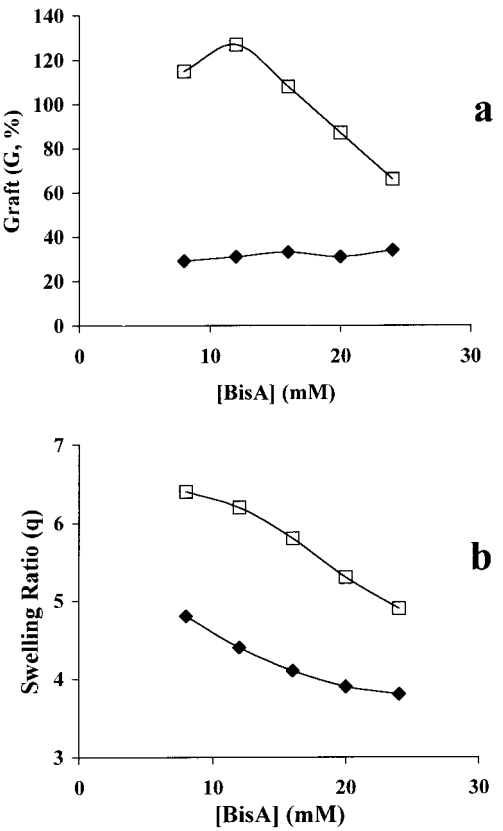


**Figure 3** Effects of the crosslinker concentration on (a) *G* and (b) *q* ([NIPAAm] = 1*M*): (♦) method I and (□) method II.

the collapse of hydrogels from drying. The hydrogel-covered fibers began to merge together at $G = 45\%$, and this phenomenon became more obvious at $G = 58\%$, at which a smooth appearance of the hydrogel was observed. With method I, the hydrogel formed was limited by the amounts of the monomer/crosslinker solutions taken up by the cellulose substrate up to the saturation level. With series I, hydro-

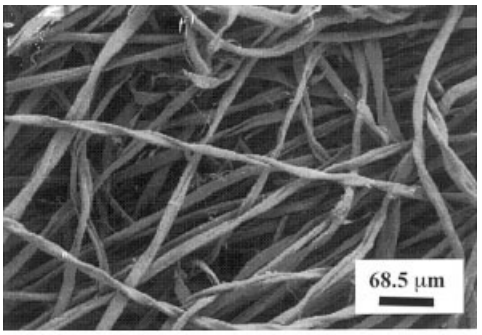


(a)

**Figure 4** SEM images of (a) hydroentangled cotton cellulose and cellulose-supported PNIPAAm hydrogels prepared by (b) method I at different *G* values (%) and (c) method II ($G = 214\%$; the surface of the gel layer is on the left, and the cross section of the whole composite is on the right).

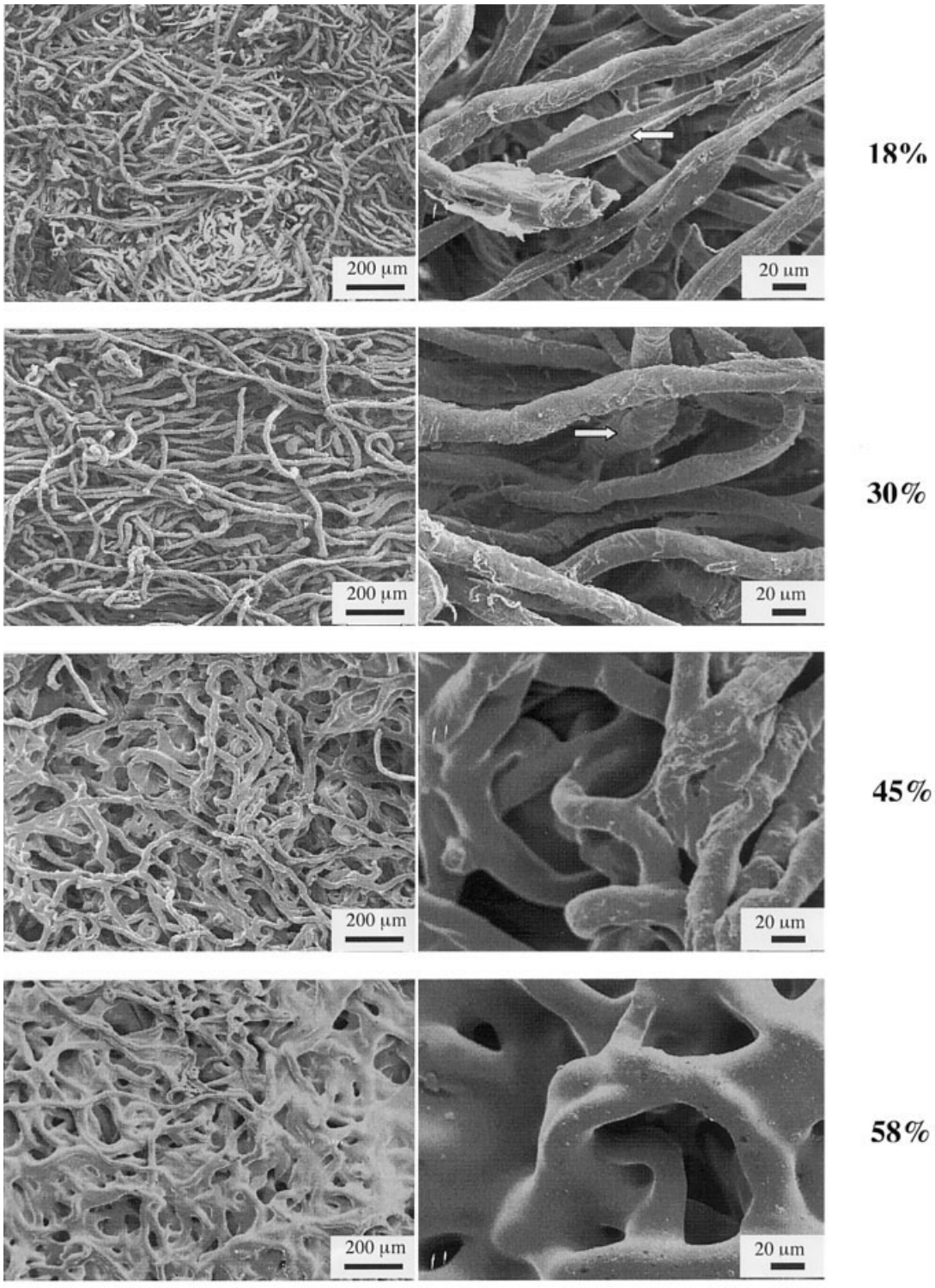


**Figure 4** (*Continued from the previous page*)

gels were formed on fiber surfaces and within the interfiber pores. It was, therefore, expected that the fiber structure and pore volume on the substrate could be affected significantly by the extent of the hydrogel grafted.

The hydrogels in composite series II were mainly bulk on the cellulose supports. In fact, very little fibrous structure could be observed in the hydrogel layer [Fig. 4(c)]. In method II, the bulk of the excessive reactant solution was outside of the solids, and the

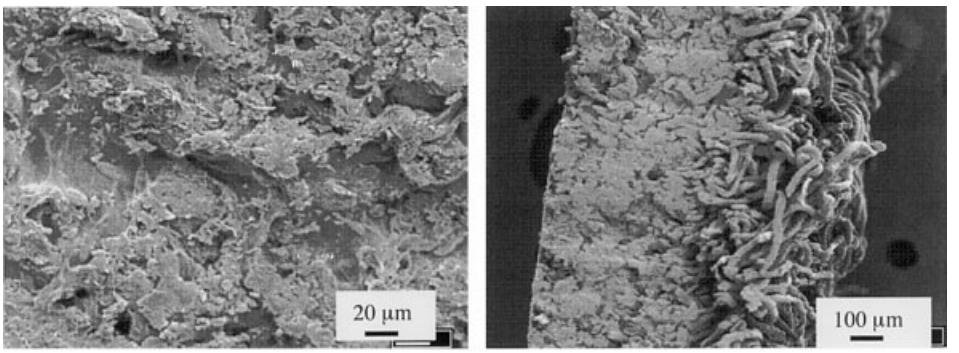


(c)

**Figure 4** (*Continued from the previous page*)

hydrogel formed was expected not to be restricted by the substrate structure. Both the amounts of the solutions and the reactant concentrations showed stronger effects on the amounts of grafted hydrogels.

The swelling behaviors from the two series, each at various NIPAAm and BisA concentrations, were examined with respect to *G*. Figure 5 shows that these two series had opposite *q*–*G* relationships. The distinctly different morphologies of these two series of hydrogel–cellullose composites help to explain their opposite swelling behaviors with respect to the levels of grafting. With series II, the hydrogels formed were located mainly outside of the interfiber pores, and their swelling behavior appeared to be less restricted by the pore structure of the solids that supported them. *q* increased with *G*. However, for series I hydrogel–cellulose composites, the main space that the hydrogel occupied and in which it expanded was the fiber surfaces and the pores between fibers. With an increasing amount of the hydrogel, there was less void volume in which the hydrogel could expand, and the swelling ability of the hydrogel decreased with increasing hydrogel. In fact, the swelling of series I hydrogel–cellulose composites was even lower than the water absorbed in the original cellulose substrate, which was 5.7 times in mass. A portion of the hydrogel (1*M* NIPAAm, 1.2% BisA) that sheared off from the surface of the hydrogel–cellulose composites (series II) was measured to have a swelling ratio of 23. This was much larger than the overall swelling ratios of any of the series II hydrogel–cellulose composites. The swelling of the hydrogels attached to a cellulose solid was expected to be lower because of the chemical linkage to the substrates.

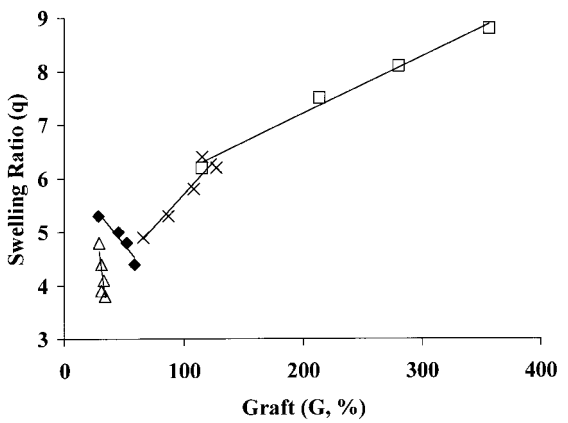


**Figure 5** Relationship between *G* and *q*: (◆,△) method I and (□,×) method II [(◆,□) varying [NIPAAm] [BisA] = 1.2% of [NIPAAm]; (△,×) varying [BisA], [NIPAAm] = 1*M*).

## Pore structure

Method I generated hydrogel-covered fibers to hydrogel-filled fibrous membranes, which represent progressively altered porous structures. SEM gave information on the morphologies in the dry state, and swelling measurements showed their behaviors in hydrated states. It would be valuable to use a single measurement to illustrate and compare the pore structural changes in the dry and swelling states. A nonswelling liquid with low surface tension and viscosity, such as hexadecane, can be used to fill available pore structures to give an estimation of the total pore volume in porous media.[26,27] As expected, the pore volume of the dry hydrogel–cellulose composites (series I) decreased with increasing grafted hydrogels (Fig. 6). In their fully hydrated states, these composites still contained some levels of voids. As for the dry state, the total pores decreased with increasing *G*. From the dry state to the swollen state, the pore volume was reduced by about two-thirds at any given *G*. These data show that the pore sizes and porosity could be controlled by the grafting level and the swelling of the hydrogels. Linear regressions of these pore volume data showed that zero porosity could be achieved with either $G = 110\%$ in the dry state or $G = 96\%$ in the fully swollen state.

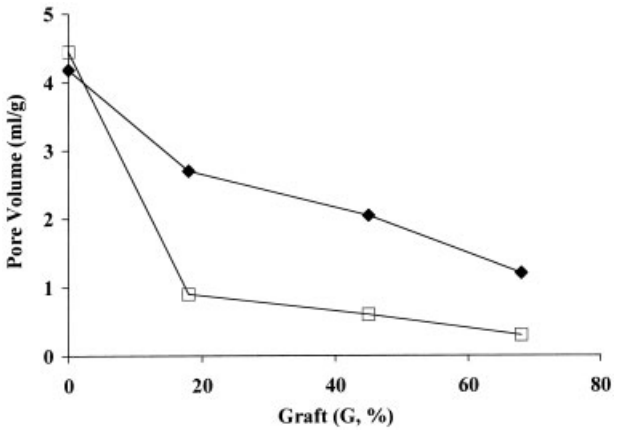


**Figure 6** Pore volumes of hydrogel composites prepared by method I in (♦) the dry state and (□) the water-swollen state.

## Phase transitions

The phase transitions of cellulose-supported hydrogels were observed with increasing temperatures above the LCST of PNIPAAm (Fig. 7). In our previous work, PNIPAAm hydrogels alone showed a distinct drop in swelling ($q$ dropped from 30 to 10) around 32°C.[27] The cellulose-supported hydrogels exhibited lower levels of deswelling over a wider temperature range. The onset temperatures of the phase-transition began near 28°C, with deswelling occurring between 28 and 40°C. The hydrogels formed with less crosslinker exhibited larger drops in $q$ in this temperature range. However, the $q$ values at the collapsed state did not appear to be affected by the levels of crosslinking.

The phase-transition behavior was also observed from the DSC endothermic peak corresponding to the deswelling of the hydrogel (Fig. 8). Again, the cellulose-supported hydrogels showed much smaller but broader endothermic peaks than the free hydrogel. The onset temperatures of the endothermic peaks of solid-supported hydrogels were between 28 and 32°C, close to the transition temperature of the free hydrogel. However, the lower the amount was of the hydrogels on cellulose, the higher the temperatures were at which the phase transitions ended. This means that it took longer to reach the deswelling equilibrium for samples with lower levels of grafted hydrogels.

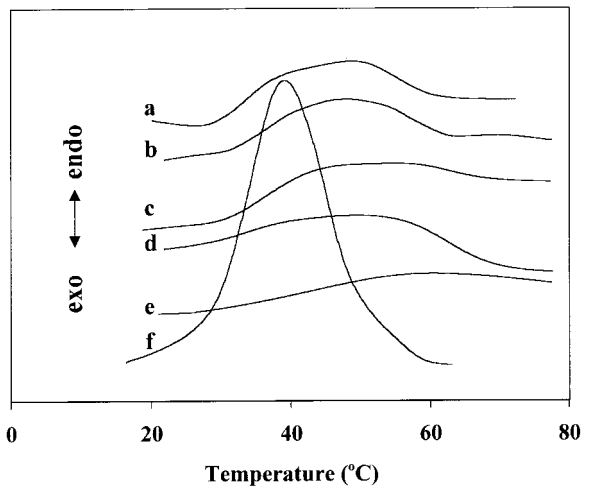


**Figure 8** DSC thermograms (kJ/g of composite) for fully swollen cellulose-supported hydrogels at various values of $G$: (a) 253% from method II, (b) 127% from method II, (c) 56% from method I, (d) 27% from method I, (e) fully hydrated cellulose, and (f) fully hydrated free hydrogel from a.

The endothermic heat for the phase transition was calculated from DSC thermograms on the basis of the masses of the hydrogels (Fig. 9). With a low $G$ value of 27%, the swelling ratio of the cellulose-supported hydrogel had a phase-transition enthalpy close to that of

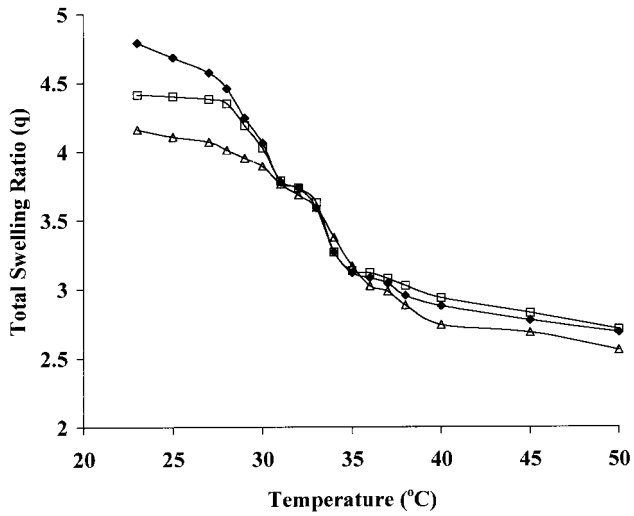


**Figure 7** Swelling of cellulose-supported PNIPAAm hydrogels ([NIPAAm] = 1*M*) from method I as a function of temperature {[BisA] = (♦) 8, (□) 16, or (△) 20 m*M*}.

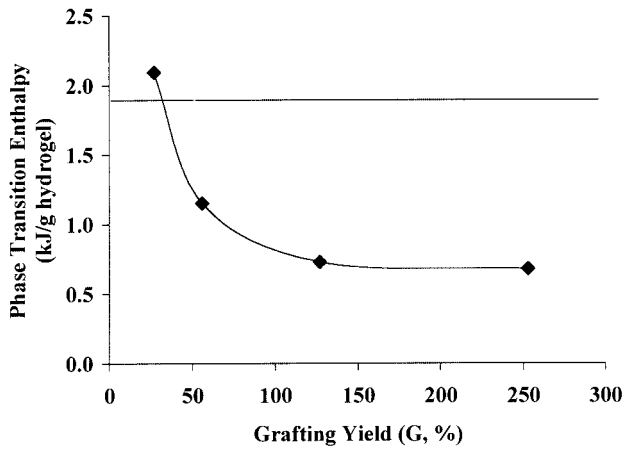


**Figure 9** Phase-transition enthalpy of hydrogels calculated from DSC thermograms. The line indicates the enthalpy of free hydrogels.

the free hydrogel. The enthalpies decreased with increasing grafts. When more hydrogel was grafted onto the substrates, there was less space for the hydrogel to expand, and it could not swell as fully as the free hydrogel. The partially swollen hydrogel had a lower phase-transition enthalpy and took less time to reach the deswelling equilibrium.

## CONCLUSIONS

This study has demonstrated that cotton cellulose can effectively be initiated with ceric ions to support the graft polymerization of thermally sensitive PNIPAAm hydrogel networks. Two series of hydrogel–cellulose composites were prepared by a two-step initiation and polymerization process, with BisA as the crosslinker. These two series exhibited distinctively different morphologies and swelling behaviors. The optimal initiation conditions for the cellulose solids involved immersing the substrates in a 20 m*M* CAN solution for 15 min. The polymerization of NIPAAm/BisA below the saturation level in the pores of the cellulose produced porous substrates (series I) with grafting generally less than 100%. The morphologies ranged from hydrogel-covered fibers to hydrogel-filled fibrous substrates. Polymerizing the NIPAAm/BisA-saturated cellulose in the presence of an excessive NIPAAm/BisA solution resulted in completely encapsulated cellulose solids (series II) in the bulk of hydrogels at a grafting level up to 400%. With both methods, the extent of grafted hydrogels increased with increasing monomer concentrations, and the overall swelling of the hydrogel–cellulose composites decreased with increasing crosslinker concentrations. The swelling behaviors of these two series of hydrogel–cellulose composites with respect to the levels of the hydrogels grafted were opposite, however, because of their distinctively different morphologies. Both series exhibited thermally responsive swelling and deswelling behaviors. These phase transitions occurred over a wider temperature range, that is, between 28 and 40°C, in comparison with the 32°C LCST of free PNIPAAm hydrogels. These initiation and polymerization procedures offer the options of reinforcing hydrogels with solid supports and preparing cellulose membranes whose pore sizes can be controlled by the swelling of hydrogels. The controlled-release behavior and thermally regulated pore size control characteristics are potentially useful in many applications, including wound-dressing materials, dialysis membranes, drug delivery carriers, and enzyme immobilization.

## References


1. Byrne, M. E.; Park, K.; Peppas, N. A. Adv Drug Delivery Rev 2002, 54, 149.
2. Hoffman, A. S. Adv Drug Delivery Rev 2002, 54, 3.
3. Peppas, N. A.; Huang, Y.; Torres-Lugo, M.; Ward, J. H.; Zhang, J. Annu Rev Biomed Eng 2000, 2, 9.
4. Karlsson, J. O.; Gatenholm, P. Polymer 1997, 38, 4727.
5. Karlsson, J. O.; Gatenholm, P. Polymer 1999, 40, 379.
6. Karlsson, J. O.; Henriksson, A.; Michalek, J.; Gatenholm, P. Polymer 1996, 41, 1551.
7. Karlsson, J. O.; Gatenholm, P. Polymer 1996, 37, 4251.
8. Karlsson, J. O.; Gatenholm, P. Macromolecules 1999, 32, 7594.
9. Liu, J.; Zhai, M.; Ha, H. Radiat Phys Chem 1999, 55, 55.
10. Li, J.; Zhai, M.; Yi, M.; Gao, H.; Ha, H. Radiat Phys Chem 1999, 55, 173.
11. Ogiwara, Y. O.; Ogiwara, Y. U.; Kubota, H. J Polym Sci Part A-1: Polym Chem 1968, 6, 1489.
12. Graczyk, T. J Appl Polym Sci 1989, 38, 619.
13. Duke, F. R.; Forist, A. A. J Am Chem Soc 1949, 71, 2790.
14. Hintz, H. L.; Johnson, D. C. J Org Chem 1967, 32, 556.
15. Mino, G.; Kaizerman, S.; Rasmussen, E. J Polym Sci 1959, 39, 523.
16. Katai, A. A.; Kulshrestha, V. K.; Marchessault, R. H. J Polym Sci Part C: Polym Symp 1963, 2, 403.
17. Ogiwara, Y. O.; Ogiwara, Y. U.; Kubota, H. J Polym Sci Part A-1: Polym Chem 1967, 5, 2791.
18. Kulkarni, A. Y.; Mehta, P. C. J Appl Polym Sci 1968, 12, 1321.
19. Iwakura, Y.; Imai, Y.; Yagi, K. J Polym Sci Part A-1: Polym Chem 1968, 6, 801.
20. Kubata, H.; Shiobara, N. React Funct Polym 1998, 37, 219.
21. Nonaka, T.; Hashimoto, K.; Kurihara, S. J Appl Polym Sci 1997, 66, 209.
22. Hebeish, A.; Guthrie, J. T. The Chemistry and Technology of Cellulosic Copolymers; Springer-Verlag: Berlin, 1981; Chapter 4.
23. Takahashi, T.; Hori, Y.; Sato, I. J Polym Sci Part A-1: Polym Chem 1968, 6, 2091.
24. Takahashi, T.; Nagata, M.; Hori, Y.; Sato, I. J Polym Sci Part B: Polym Lett 1967, 5, 509.
25. Hsieh, Y.-L.; Yu, B. Text Res J 1992, 62, 677.
26. Hsieh, Y.-L. Text Res J 1995, 65, 299.
27. Zhou, W.-J.; Kurth, M. J.; Hsieh, Y.-L.; Krochta, J. M. J Polym Sci Part A: Polym Chem 1999, 37, 1393.